ChemComm

COMMUNICATION

View Article Online
View Journal

Cite this: DOI: 10.1039/d4cc03892d

Received 1st August 2024,
Accepted 24th September 2024

DOI: 10.1039/d4cc03892d

rsc.li/chemcomm

Photoswitchable TCB-2 for control of the 5-HT$_{2A}$ receptor and analysis of biased agonism†

Alireza Jafar Esmaeili,‡ Pantea Montazeri,‡ Jasmine Cristina Gomez, Didier J. Dumervil, Faezeh Safar Nezhad and Rachel C. Steinhardt *

Therapies that target the serotonin 2A receptor (5-HT$_{2A}$R) are promising. However, probes are needed to better understand the role of 5-HT$_{2A}$R. Here, we design and synthesize a photoswitch and photoswitchable 5-HT$_{2A}$R ligand based on highly potent agonist TCB-2 and arylazopyrazole, which also boasts photoswitchable G protein *vs.* β-arrestin pathway bias.

Serotonin is required for manifold processes throughout the body, ranging from homeostasis and digestion to complex central nervous function. There are 14 subtypes of serotonin receptor, and stemming their importance in biological processes such as cognition and mood, there has been intense focus on developing new drugs and probes for this receptor family.[1–3] Recently, agonists of the 5-HT$_{2A}$R have generated intense interest. Specifically, psychedelic compounds like psilocybin are under study for treatment of disease ranging from anxiety, depression, obsessive-compulsive disorder, to substance use disorder.[4–10] However, these drugs are also active at many neurologically important monoamine receptors. The precise role of 5-HT$_{2A}$R in the dramatic and potentially long-ranging benefits of these therapeutic interventions remains unclear and under intense study.[10–19]

To understand 5-HT$_{2A}$R's therapeutic potential, new selective probes are needed. Here we develop a photopharmacological probe for 5-HT$_{2A}$R based on the subtype selective and highly potent ligand TCB-2.[20,21] Such probes provide spatial and temporal precision.[22,23] There only a couple of such 5-HT$_{2A}$R probes known, and ours is the first to be based on such a selective ligand.[24,25] TCB-2 is a high affinity ligand for 5-HT$_{2A}$R, with a potency analogous to lysergic acid diethylamide (LSD).[20] It is a member of a family of synthetic mescaline derivatives based on the 2,5-methoxyphenethylamine scaffold, where it is known that lipophilic substituents at the 4′ position of the aryl ring confer increased potency at 5-HT$_{2A}$R (Fig. 1).[26] Among this family are the class of *N*-benzylated derivatives known as the *N*-benzyl phenethylamine (NBOMe) which contains some of the most potent and selective 5-HT$_{2A}$R ligands known (Fig. 1).[19,26,27]

With this information in mind, we designed a 5-HT$_{2A}$R probe *via* *N*-arylating TCB-2 with a photoswitch (Fig. 1). We hypothesized that the change in sterics by isomerization of the extended pi system of the switch would lead to altered activity at the receptor. Additionally, we wanted to determine whether the large volume change of photoswitching would alter the signalling bias of 5-HT$_{2A}$R.[28] "Bias" refers to the fact that 5-HT$_{2A}$R can signal *via* multiple pathways, and crucially for drug design, 5-HT$_{2A}$R can interact with the G protein or β-arrestin2 pathways.[29–31] These pathways known to induce dramatically different physiological effects for other GPCRs, and it is hypothesized that these pathways differentially contribute to the psychedelic and therapeutic effects of psychedelic drugs.[10,17,32–34] This area is currently under study and more work is needed to clarify the biochemistry of these pathway contributions. There are only two biased photoswitchable ligands reported so far, Broichhagen *et al.* reported on a photoswitching probe "LirAzo" with biased functionality at GLP-1R, and the Decker group disclosed a biased photoswitching cannabinoid 2 receptor agonist.[35,36]

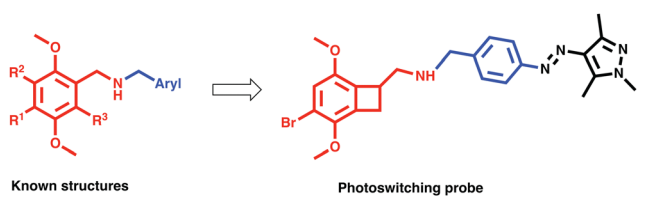

Fig. 1 Left: Structures of known derivatives of 2,5-methoxyphenethylamine (red) and NBOMe family (blue + red), for NBOMe family R^1 = Br, I, CF$_3$, CN, Me, linear alkyl, *O*-alkyl, *S*-alkyl, R^2, R^3 = H. Right: The shared skeletal components mapped onto the photoswitching probe.

Syracuse University, Department of Chemistry, 111 College Pl., Syracuse, NY 13244, USA. E-mail: rcsteinh@syr.edu

† Electronic supplementary information (ESI) available. See DOI: https://doi.org/10.1039/d4cc03892d

‡ These authors contributed equally to this work.

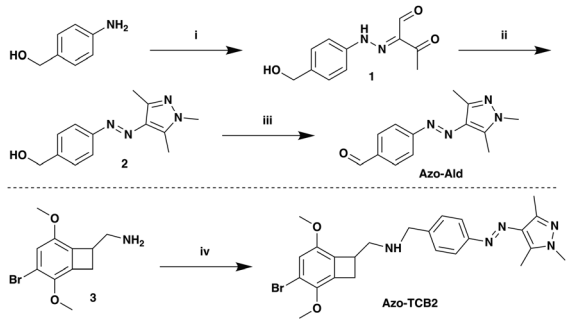

Scheme 1 Synthesis of **Azo-Ald** and **Azo-TCB2** (i) sodium nitrite, 2,4-pentanedione, AcOH, HCl, H_2O, NaOAc, 0 °C → RT 12 h, 42%. (ii) Methylhydrazine, EtOH, reflux, 2.5 h, 50%. (iii) MnO_2 (activated), $CHCl_3$, RT, 12 h, 78% (iv) **Azo-Ald**, $NaCNBH_3$, 79%.

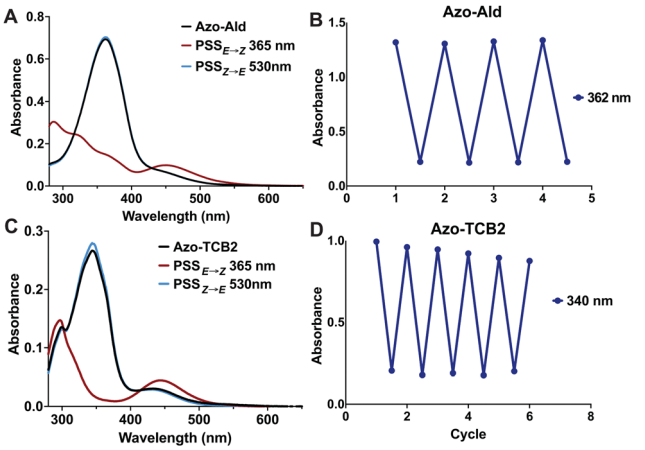

Fig. 2 (A) Photoisomerization of **Azo-Ald** after irradiation with 365 nm light (red), 530 nm light, or at dark thermal equilibrium (black). (B) Switching irradiation cycles (30 seconds) to determine photofatigue of **Azo-Ald**. (C) Photoisomerization of **Azo-TCB2** after irradiation with 365 nm light (red), 530 nm light, or at dark thermal equilibrium (black) (D) switching irradiation cycles (30 seconds) to determine photofatigue of **Azo-TCB2**.

For the photoswitch identity, we chose an arylazopyrazole (AAP), due to its excellent photophysical and photochemical properties, and well-documented use in biological systems.[23,37–41] For the present application we synthesized a novel AAP, **Azo-Ald** (Scheme 1), for ease of installation *via* reductive amination. We modified the electronics of the pyrazole ring based on the findings of the Fuchter group.[42]

The syntheses of **Azo-Ald** and **Azo-TCB2** began with commercially available 4-aminobenzyl alcohol, which was first diazotized with sodium nitrite in acetic and HCl, followed by diazo coupling with the enolate of 2,4-pentanedione to furnish hydrazone **1**.[43,44] The product was then condensed with methylhydrazine to provide pyrazole **2**.[44,45] The benzylic alcohol on **2** was readily oxidized using activated MnO_2 to provide **Azo-Ald**. The drug TCB-2 was incubated with **Azo-Ald**, followed by the addition of sodium cyanoborohydride to yield the reductive amination product **Azo-TCB2**.

Next, we investigated the photophysical properties of **Azo-Ald** and **Azo-TCB2** using UV/Vis spectroscopy and ^{1}H NMR. Solutions were prepared in 22 μM solution in DMSO, and a UV transilluminator was used to provide the 365 nm irradiation for $E \rightarrow Z$ conversion, and a 530 nm LED (Thorlabs) was used for the $Z \rightarrow E$ conversion. Photostationary states (PSS) were determined by ^{1}H NMR and the UV/Vis spectra were recorded both at the dark equilibrated and PSS states, with the dark states showing absorbance maxima at 362 nm for **Azo-Ald** and 340 nm for **Azo-TCB2** and PSSs with absorption maxima at 446 nm and 440 nm, this well resolved wavelength shift also reveals isosbestic points at ∼400 nm for both compounds (Fig. 2a and c). Both **Azo-Ald** and **Azo-TCB2** showed good fatigue resistance over multiple switching cycles (Fig. 2b and d).

NMR spectroscopy showed that after irradiation at 365 nm the $PSS_{E\to Z}$ for **Azo-Ald** in DMSO at was 62%, this was improved to 98% for **Azo-TCB2**. This may be due to the presence of an electron-donating group at the *para* position of the benzene ring. The rate of thermal relaxation of the less stable *E*-state was then investigated and showed that **Azo-TCB2** has good potential for *in vivo* use, due to its 29.14 h half-life at 25 °C (Table 1) and 21.01 h half life at 37 °C. These photophysical data showed that

Table 1 Photophysical properties of **Azo-Ald** and **Azo-TCB2** at 25 °C

Ligand	PSS_{E-Z} (%*Z*)	PSS_{Z-E} (%*E*)	$t_{1/2}$ *Z* isomer	ϕ_{E-Z} (%)	ϕ_{Z-E} (%)
Azo-Ald	62	100	11 minutes	0.13	0.36
Azo-TCB2	98	83	29.14 hours	0.26	0.24

Azo-TCB2 was an effective photoswitch meriting investigation of its biochemical parameters.

We next analysed the binding of **Azo-TCB2** at the 5-HT_{2A} receptor *via* assays for G-protein and β-arrestin pathway activation. G-protein mediated signalling by 5-HT_{2A} was determined by intracellular calcium measurement. The assay functions by measurement of changes in intracellular calcium flux *via* imaging of a ratiometric calcium-binding fluorescent dye. To perform the assay, HEK293T cells were transfected with 5-HT_{2A}, followed by loading with the calcium-sensing dye Cal-590™AM. Ligand binding to 5-HT_{2A}R results in an influx of calcium in the cytoplasm, which is monitored in real time by confocal imaging of the increase in calcium sensor fluorescence.

The live cell imaging calcium flux data (Fig. 3) shows that **Azo-TCB2** pharmacophore activates 5-HT_{2A} in a dose-dependent fashion in the *E* and *Z* states, with a relative increase in maximal partial agonism in the photoswiched *Z* state. Comparison of EC_{50} curves between the two states shows the *Z* state with ≈ 2,4-fold increase in EC_{50} over the *E* state. In the *Z* state, the orientation of the arylpyrazole group decreases the receptor's maximal response to **Azo-TCB2** relative to TCB-2, rendering this isomer an apparent partial agonist as compared to the apparent full agonism of the *E* isomer. Statistical analysis of the two curves using ordinary one-way ANOVA (analysis of variance) shows statistically significant differences between the higher concentrations of the *E* and *Z* states. Both *E* and *Z* forms have good potency at the receptor, with EC_{50} of 22.8 nM nm and 46.7 nM respectively, compared to our measured 5.9 nM nm for the positive control, which is in

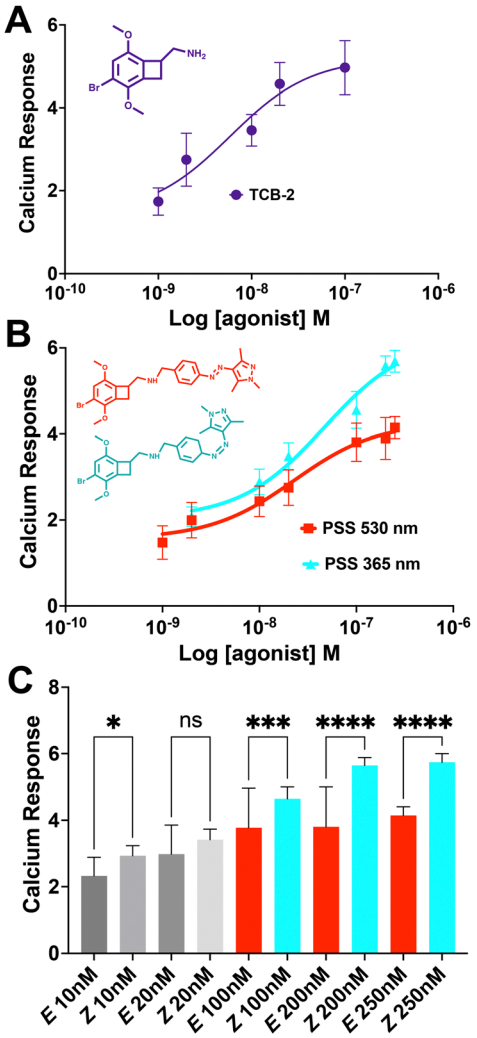

Fig. 3 (A) Dose response of 5-HT_{2A}R to TCB-2 in the fluorescent live cell Ca^{2+} assay EC_{50} = 5.9 nM, nonlinear regression curve fit R^2 = 0.94. (B) Dose response of 5-HT_{2A} to *E vs. Z* states, *E* EC_{50} = 22.8 nM, nonlinear regression curve fit R^2 = 0.98; *Z* EC_{50} = 46.7 nM, nonlinear regression curve fit R^2 = 0.98. (C) Statistical analysis of differences in Ca^{2+} response between *E* and *Z* states for individual concentrations. *$p < 0.05$, ***$p < 0.0005$, ****$p < 0.0001$, one-way ANOVA (analysis of variance). Error bars represent mean ± standard deviation, data shown is result of 3 independent experiments, with an *n* of at least 20 cells for each point.

agreement with the literature value of 0.75 nM.[20] This indicates a rightward shift in agonism, and thus relative decrease in potency *vs.* the parent compound, TCB-2. Overall, these data indicate that in the context of the G-protein pathway, the *E* and *Z* states are both still excellent at initiating a Ca^{2+} response, and photoswitching **Azo-TCB2** results in a decrease in EC_{50} and maximal response. With this information in hand, we next sought to determine the 5-HT_{2A}R β-arrestin response.

The response of the β-arrestin effector pathway was characterized with the parallel-receptor-ome expression and screening *via* transcriptional output TANGO (PRESTO–TANGO) assay developed in the Roth lab.[46,47] This assay monitors β-arrestin activity by expression of a luciferase reporter gene. The β-arrestin recruitment data showed some notable differences

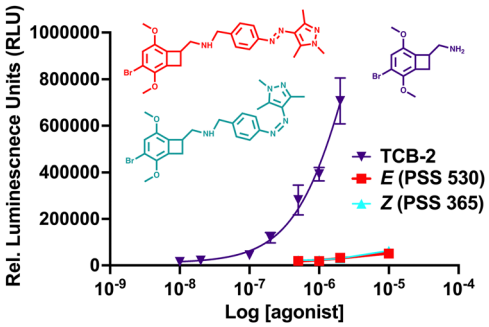

Fig. 4 Dose response of 5-HT_{2A}R β-arrestin recruitment for TCB-2 and the *E vs. Z* states, TCB-2 EC_{50} = 3.7 μM, nonlinear regression curve fit R^2 = 0.96; *E* EC_{50} = 3.5 μM, nonlinear regression curve fit R^2 = 0.90; *Z* EC_{50} = 43.3 μM, nonlinear regression curve fit R^2 = 0.96. Error bars represent mean ± standard deviation from 4 replicates.

compared to the G-protein pathway. For the isomers, data (Fig. 4), show that both *E* and *Z* states are rendered apparent partial agonists of 5-HT_{2A}R, with ≈14-fold difference in maximal response between the two isomers and that of the parent compound. In terms of potency, the *E* state retains an EC_{50} equivalent to the parent compound, while the *Z* state differed, and both are greatly decreased in maximal response.

Next, we analysed the differential initiation of G-protein *vs.* β-arrestin pathways for the **Azo-TCB2** (Fig. 5). To quantify pathway bias for the two states, we first converted each isomer's response to percent of the reference compound's maximal response, with TCB-2 serving as the reference compound. From comparing these numbers, we can see that the predominantly *Z* compound has become more β-arrestin pathway biased *vs.* the predominantly *E*.

In conclusion, here we have described one of the first photoswtiching probes for 5-HT_{2A}R, and the first to demonstrate switchable pathway bias. There is differential potency between the two isomers in the G-protein pathway, while the potencies are similar in the β-arrestin pathway. The isomers have excellent photophysical parameters such as low rate of thermal back switching and fatigue resistance. Additionally, this work provides medicinal chemistry data on this structural class which is of intense biomedical interest, specifically on the sensitivity to substitution with extended *N*-aryl groups.[27,33] In future steps, this probe can be used in studies towards

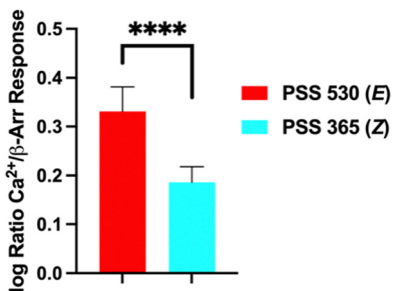

Fig. 5 Agonism bias for **Azo-TCB2** isomers. ****$p < 0.0001$, Student's *t*-test. Error bars represent mean ± standard deviation.

treating diseases ranging from anxiety, depression, obsessive-compulsive disorder, to substance use disorder.[4–10] This probe can also contribute to the fundamental untangling of the G-protein and β-arrestin pathway contributions to therapeutic effects.

The authors wish to thank the National Science Foundation, award # 2238400.

Data availability

The data supporting this article have been included as part of the ESI.†

Conflicts of interest

There are no conflicts to declare.

Notes and references

1 D. E. Nichols and C. D. Nichols, *Chem. Rev.*, 2008, **108**, 1614–1641.
2 M. Berger, J. A. Gray and B. L. Roth, *Annu. Rev. Med.*, 2009, **60**, 355–366.
3 J. D. McCorvy and B. L. Roth, *Pharmacol. Ther.*, 2015, **150**, 129–142.
4 R. L. Carhart-Harris, M. Bolstridge, C. M. J. Day, J. Rucker, R. Watts, D. E. Erritzoe, M. Kaelen, B. Giribaldi, M. Bloomfield, S. Pilling, J. A. Rickard, B. Forbes, A. Feilding, D. Taylor, H. V. Curran and D. J. Nutt, *Psychopharmacology*, 2018, **235**, 399–408.
5 P. A. Davoudian, L.-X. Shao and A. C. Kwan, *ACS Chem. Neurosci.*, 2023, **14**, 468–480.
6 R. R. Griffiths, M. W. Johnson, M. A. Carducci, A. Umbricht, W. A. Richards, B. D. Richards, M. P. Cosimano and M. A. Klinedinst, *J. Psychopharmacol.*, 2016, **30**, 1181–1197.
7 C. L. Raison, G. Sanacora, J. Woolley, K. Heinzerling, B. W. Dunlop, R. T. Brown, R. Kakar, M. Hassman, R. P. Trivedi, R. Robison, N. Gukasyan, S. M. Nayak, X. Hu, K. C. O'Donnell, B. Kelmendi, J. Sloshower, A. D. Penn, E. Bradley, D. F. Kelly, T. Mletzko, C. R. Nicholas, P. R. Hutson, G. Tarpley, M. Utzinger, K. Lenoch, K. Warchol, T. Gapasin, M. C. Davis, C. Nelson-Douthit, S. Wilson, C. Brown, W. Linton, M. W. Johnson, S. Ross and R. R. Griffiths, *JAMA*, 2023, **330**, 843.
8 R. L. Carhart-Harris and G. M. Goodwin, *Neuropsychopharmacology*, 2017, **42**, 2105–2113.
9 T. Chi and J. A. Gold, *J. Neurol. Sci.*, 2020, **411**, 116715.
10 W. Duan, D. Cao, S. Wang and J. Cheng, *Chem. Rev.*, 2024, **124**, 124–163.
11 M. Hibicke, A. N. Landry, H. M. Kramer, Z. K. Talman and C. D. Nichols, *ACS Chem. Neurosci.*, 2020, **11**, 864–871.
12 L. P. Cameron, S. D. Patel, M. V. Vargas, E. V. Barragan, H. N. Saeger, H. T. Warren, W. L. Chow, J. A. Gray and D. E. Olson, *ACS Chem. Neurosci.*, 2023, **14**, 351–358.
13 D. A. Martin and C. D. Nichols, *EBioMedicine*, 2016, **11**, 262–277.
14 M. V. Vargas, L. E. Dunlap, C. Dong, S. J. Carter, R. J. Tombari, S. A. Jami, L. P. Cameron, S. D. Patel, J. J. Hennessey, H. N. Saeger, J. D. McCorvy, J. A. Gray, L. Tian and D. E. Olson, *Science*, 2023, **379**, 700–706.
15 D. E. Olson, *ACS Pharmacol. Transl. Sci.*, 2021, **4**, 563–567.
16 D. B. Yaden and R. R. Griffiths, *ACS Pharmacol. Transl. Sci.*, 2021, **4**, 568–572.
17 J. F. López-Giménez and J. González-Maeso, in *Behavioral Neurobiology of Psychedelic Drugs*, ed. A. L. Halberstadt, F. X. Vollenweider and D. E. Nichols, Springer Berlin Heidelberg, Berlin, Heidelberg, 2017, vol. 36, pp. 45–73.
18 D. E. Olson, *Biochemistry*, 2022, **61**, 127–136.
19 J. Wallach, A. B. Cao, M. M. Calkins, A. J. Heim, J. K. Lanham, E. M. Bonniwell, J. J. Hennessey, H. A. Bock, E. I. Anderson, A. M. Sherwood, H. Morris, R. De Klein, A. K. Klein, B. Cuccurazzu, J. Gamrat, T. Fannana, R. Zauhar, A. L. Halberstadt and J. D. McCorvy, *Nat. Commun.*, 2023, **14**, 8221.
20 T. H. McLean, J. C. Parrish, M. R. Braden, D. Marona-Lewicka, A. Gallardo-Godoy and D. E. Nichols, *J. Med. Chem.*, 2006, **49**, 5794–5803.
21 M. A. Fox, H. T. French, J. L. LaPorte, A. R. Blackler and D. L. Murphy, *Psychopharmacology*, 2010, **212**, 13–23.
22 J. Broichhagen, J. A. Frank and D. Trauner, *Acc. Chem. Res.*, 2015, **48**, 1947–1960.
23 M. J. Fuchter, *J. Med. Chem.*, 2020, **63**, 11436–11447.
24 H. Gerwe, F. He, E. Pottie, C. Stove and M. Decker, *Angew. Chem., Int. Ed.*, 2022, **61**, e202203034.
25 J. Morstein, G. Romano, B. E. Hetzler, A. Plante, C. Haake, J. Levitz and D. Trauner, *Angew. Chem., Int. Ed.*, 2022, **62**, e202117094.
26 E. M. Rørsted, A. A. Jensen, G. Smits, K. Frydenvang and J. L. Kristensen, *J. Med. Chem.*, 2024, **67**, 7224–7244.
27 E. Märcher Rørsted, A. A. Jensen and J. L. Kristensen, *ChemMedChem*, 2021, **16**, 3263–3270.
28 A. Gonzalez, E. S. Kengmana, M. V. Fonseca and G. G. D. Han, *Mater. Today Adv.*, 2020, **6**, 100058.
29 E. Reiter, S. Ahn, A. K. Shukla and R. J. Lefkowitz, *Annu. Rev. Pharmacol. Toxicol.*, 2012, **52**, 179–197.
30 J. S. Smith, R. J. Lefkowitz and S. Rajagopal, *Nat. Rev. Drug Discovery*, 2018, **17**, 243–260.
31 J. W. Wisler, H. A. Rockman and R. J. Lefkowitz, *Circulation*, 2018, **137**, 2315–2317.
32 E. Pottie, C. B. M. Poulie, I. A. Simon, K. Harpsøe, L. D'Andrea, I. V. Komarov, D. E. Gloriam, A. A. Jensen, J. L. Kristensen and C. P. Stove, *ACS Chem. Neurosci.*, 2023, **14**, 2727–2742.
33 C. B. M. Poulie, E. Pottie, I. A. Simon, K. Harpsøe, L. D'Andrea, I. V. Komarov, D. E. Gloriam, A. A. Jensen, C. P. Stove and J. L. Kristensen, *J. Med. Chem.*, 2022, **65**, 12031–12043.
34 E. Pottie and C. P. Stove, *J. Neurochem.*, 2022, **162**, 39–59.
35 J. Broichhagen, T. Podewin, H. Meyer-Berg, Y. vonOhlen, N. R. Johnston, B. J. Jones, S. R. Bloom, G. A. Rutter, A. Hoffmann-Röder, D. J. Hodson and D. Trauner, *Angew. Chem., Int. Ed.*, 2015, **54**, 15565–15569.
36 S. A. M. Steinmüller, J. Fender, M. H. Deventer, A. Tutov, K. Lorenz, C. P. Stove, J. N. Hislop and M. Decker, *Angew. Chem., Int. Ed.*, 2023, **62**, e202306176.
37 C. E. Weston, A. Krämer, F. Colin, Ö. Yildiz, M. G. J. Baud, F.-J. Meyer-Almes and M. J. Fuchter, *ACS Infect. Dis.*, 2017, **3**, 152–161.
38 L. Stricker, M. Böckmann, T. M. Kirse, N. L. Doltsinis and B. J. Ravoo, *Chem. – Eur. J.*, 2018, **24**, 8639–8647.
39 P. Kobauri, F. J. Dekker, W. Szymanski and B. L. Feringa, *Angew. Chem., Int. Ed.*, 2023, **62**, e202300681.
40 J. Volarić, W. Szymanski, N. A. Simeth and B. L. Feringa, *Chem. Soc. Rev.*, 2021, **50**, 12377–12449.
41 A. K. Gaur, D. Gupta, A. Mahadevan, P. Kumar, H. Kumar, D. N. Nampoothiry, N. Kaur, S. K. Thakur, S. Singh, T. Slanina and S. Venkataramani, *J. Am. Chem. Soc.*, 2023, **145**, 10584–10594.
42 J. Calbo, A. R. Thawani, R. S. L. Gibson, A. J. P. White and M. J. Fuchter, *Beilstein J. Org. Chem.*, 2019, **15**, 2753–2764.
43 T. M. Courtney, T. J. Horst, C. P. Hankinson and A. Deiters, *Org. Biomol. Chem.*, 2019, **17**, 8348–8353.
44 J. Simke, T. Bösking and B. J. Ravoo, *Org. Lett.*, 2021, **23**, 7635–7639.
45 T. M. Courtney, T. J. Horst, C. P. Hankinson and A. Deiters, *Org. Biomol. Chem.*, 2019, **17**, 8348–8353.
46 W. K. Kroeze, M. F. Sassano, X.-P. Huang, K. Lansu, J. D. McCorvy, P. M. Giguère, N. Sciaky and B. L. Roth, *Nat. Struct. Mol. Biol.*, 2015, **22**, 362–369.
47 G. Barnea, W. Strapps, G. Herrada, Y. Berman, J. Ong, B. Kloss, R. Axel and K. J. Lee, *Proc. Natl. Acad. Sci. U. S. A.*, 2008, **105**, 64–69.

